RESEARCH PAPER

A plug-based microfluidic system for dispensing lipidic cubic phase (LCP) material validated by crystallizing membrane proteins in lipidic mesophases

**Liang Li · Qiang Fu · Christopher A. Kors ·
Lance Stewart · Peter Nollert · Philip D. Laible ·
Rustem F. Ismagilov**

Abstract This article presents a plug-based microfluidic system to dispense nanoliter-volume plugs of lipidic cubic phase (LCP) material and subsequently merge the LCP plugs with aqueous plugs. This system was validated by crystallizing membrane proteins in lipidic mesophases, including LCP. This system allows for accurate dispensing of LCP material in nanoliter volumes, prevents inadvertent phase transitions that may occur due to dehydration by enclosing LCP in plugs, and is compatible with the traditional method of forming LCP material using a membrane protein sample, as shown by the successful crystallization of bacteriorhodopsin from *Halobacterium salinarum*. Conditions for the formation of LCP plugs were characterized and presented in a phase diagram. This system was also implemented using two different methods of introducing the membrane protein: (1) the traditional method of generating the LCP material using a membrane protein sample and (2) post LCP-formation incorporation (PLI), which involves making LCP material without protein, adding the membrane protein sample externally to the LCP material, and allowing the protein to diffuse into the LCP material or into other lipidic mesophases that may result from phase transitions. Crystals of bacterial photosynthetic reaction centers from *Rhodobacter sphaeroides* and *Blastochloris viridis* were obtained using PLI. The plug-based, LCP-assisted microfluidic system, combined with the PLI method for introducing membrane protein into LCP, should be useful for minimizing consumption of samples and broadening the screening of parameter space in membrane protein crystallization.

Keywords Droplet · Plugs · Lipidic cubic phase · Membrane protein · Protein crystallization

L. Li · Q. Fu · R. F. Ismagilov (✉)
Department of Chemistry and Institute for Biophysical
Dynamics, The University of Chicago, 929 East 57th Street,
Chicago, IL 60637, USA
e-mail: r-ismagilov@uchicago.edu

C. A. Kors · P. D. Laible
Biosciences Division, Argonne National Laboratory, 9700 South
Cass Ave., Argonne, IL 60439, USA

L. Stewart
deCODE biostructures, Accelerated Technologies Center
for Gene to 3D Structure, 7869 NE Day Rd. W,
Bainbridge Island, WA 98110, USA

P. Nollert
Emerald BioSystems, Inc., 7869 NE Day Rd. W,
Bainbridge Island, WA 98110, USA

1 Introduction

This article describes a novel procedure to manipulate viscous lipidic cubic phase (LCP) material in a plug-based microfluidic system for crystallizing membrane proteins. Obtaining high quality crystals of membrane proteins is important for determining their structures (Ostermeier and Michel 1997). Purification and crystallization of membrane proteins in detergent solutions may lead to reduced activity and poor stability of the proteins. On the other hand, using a lipidic mesophase, such as LCP, is an important route to the crystallization of membrane proteins because the lipidic mesophase provides an environment similar to the natural environment of membrane proteins (Caffrey 2000). Crystallization in LCP material has been shown to be an important approach for obtaining high quality crystals of

membrane proteins, as demonstrated by the recently determined structures for two G protein-coupled receptors (Cherezov et al. 2007; Jaakola et al. 2008).

Current developments in LCP-based microscale protein crystallization include the development of robotic systems that allow for accurate handling of small amounts of LCP material (Cherezov and Caffrey 2006; Peddi et al. 2007; Perry et al. 2009) and the development of a sparse matrix screening kit, which involved pre-mixing different precipitants with monoolein to make lipidic sponge phase material (Wohri et al. 2008). Yet, crystallization in LCP material has still not been widely applied to crystallization. One reason is because LCP material has high viscosity, which makes it difficult to dispense with high accuracy using traditional tools for dispensing liquids. Furthermore, because dehydration of LCP material using conventional dispensing methods (Cherezov et al. 2004; Nollert 2002) can lead to phase transitions, current methods for working with small volumes of LCP material must be performed at high humidity to account for water loss. As each experimental setup may require a specific humidity, these methods can be complicated, take a long time, and, if carried out in parallel for a variety of conditions, alter the desired composition of the crystallization cocktail.

Recently, a microfluidic system using pneumatic valves which formed LCP material on-chip at volumes below 20 nl was developed for crystallization of membrane proteins (Perry et al. 2009). However, this system used PDMS to create the pneumatic valves, and PDMS may cause unwanted evaporation and loss of chemicals in crystallization trials, such as lipids (Toepke and Beebe 2006). Like the pneumatic valve system, the plug-based microfluidic system (Song et al. 2003, 2006a) that has been developed for protein crystallization (Lau et al. 2007; Shim et al. 2007; Zheng et al. 2005; Zheng et al. 2003) accurately handles nanoliter volumes of viscous fluids in microfluidic channels. The plug-based system has been demonstrated with clotted blood (Song et al. 2006b) and solutions containing nanoparticles (Shestopalov et al. 2004). Unlike the pneumatic valve system, using plug-based microfluidics eliminates loss of chemicals in crystallization trials as well as unwanted evaporation that can lead to phase transitions. Moreover, the plug-based microfluidic system offers the ability to simultaneously handle small volumes of different precipitants and manipulate their concentrations with high precision by using the hybrid method (Li et al. 2006).

In this article, we extend the plug-based microfluidic system to manipulation of LCP material. We demonstrated the formation of nanoliter-volume LCP plugs and the ability to merge those plugs into aqueous plugs. We then validated the developed system by crystallizing
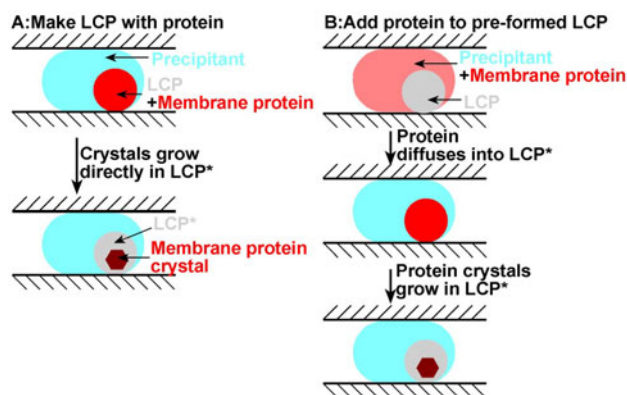

Fig. 1 Schematic showing two different methods to crystallize membrane proteins in LCP material. **a** Traditional method: the LCP material is made with protein. **b** Post LCP-formation incorporation (PLI): the LCP material is made without protein, then a membrane protein sample is added externally and allowed to diffuse into the LCP material for crystallization. * In experiments with certain precipitants, the LCP material may transform into other lipidic mesophase materials, as a result of a phase transition induced by the precipitants

membrane proteins. We introduced membrane protein samples into LCP by using two different methods: (1) the traditional method of generating the LCP material using a membrane protein sample (Fig. 1a) and (2) post LCP-formation incorporation (PLI), in which a membrane protein sample is combined with the LCP material and allowed to diffuse into the LCP material (Fig. 1b) or into other lipidic mesophases, which may result from phase transitions induced by certain precipitants, such as Jeffamine M-600 (Wadsten et al. 2006; Wohri et al. 2008). We successfully crystallized bacteriorhodopsin (BR) from *Halobacterium salinarum* using the traditional method, and we successfully crystallized the bacterial photosynthetic reaction center (RC) from two strains of *Rhodobacter sphaeroides*-a carotenoid-containing strain (Davis et al. 1988) and a carotenoidless strain (Theiler et al. 1984)-as well as RC from *Blastochloris viridis*, using PLI.

2 Materials and methods

2.1 Chemicals

All solvents and salts purchased from commercial sources were used as received unless otherwise stated. Lauryl-dimethylamine *n*-oxide (LDAO) and *n*-octyl-*β*-glucopyranoside (OG) were purchased from Anatrace (Maumee, OH). 9-Monoolein was obtained from Nu-Check Prep, Inc. (Elysian, MN). (tridecafluoro-1,1,2,2,-tetrahydrooctyl)-1 trichlorosilane was obtained from United Chemical

Technologies, Inc. (Bristol, PA). Poly(dimethylsiloxane) (Sylgard 184 Silicone Elastomer kit) was obtained from Dow Corning (Midland, MI). FC-40, a mixture of perfluoro-tri-n-butylamine and perfluoro-di-*n*-butylmethylamine, and FC-70, perfluorotripentylamine, were obtained from 3 M (St. Paul, MN).

2.2 Equipment

Spectra were analyzed using a UV–visible spectrometer purchased from Agilent (Santa Clara, CA). Teflon tubing (O.D. 250 μm, I.D. 200 μm) and Teflon tubing (O.D. 250 μm, I.D. 100 μm) were purchased from Zeus (Orangeburg, SC). Teflon tubing (O.D. 750 μm, I.D. 300 μm) was obtained from Weico Wire & Cable (Edgewood, NY). Standard wall glass tubing was obtained from Chemglass (Vineland, NJ). Gastight syringes were obtained from Hamilton Company (Reno, NV).

2.3 Fabricating PDMS devices

All microfluidic devices were fabricated from poly(dimethylsiloxane) (PDMS). Microchannels with rectangular cross sections were fabricated by using rapid prototyping (Duffy et al. 1998). The channel walls were modified with (tridecafluoro-1,1,2,2-tetrahydrooctyl)-1-trichlorosilane to increase their hydrophobicity and fluorophilicity (Roach et al. 2005).

2.4 Assembling the microfluidic system

The microfludic system consisted of two devices: one was a flow-focusing device that generated LCP plugs (Fig. 2a, b), and the other was a merging device in which aqueous plugs were formed and then merged with LCP plugs (Fig. 2c). A piece of Teflon tubing (O.D. 250 μm, I.D. 100 μm, 7–10 cm in length) was used to connect the two devices. To prevent the LCP plugs from contacting the PDMS channels, one end of the tubing was inserted through the outlet flush with the cross junction of the flow-focusing device (Fig. 2b), and the other end was inserted flush with the junction where aqueous plugs were formed via the fluorocarbon inlet of the merging device (Fig. 2c). At the junction, the Teflon tubing is wetted preferentially by FC-70, allowing LCP plugs to be formed and transported. Through the outlet of the merging device, another piece of Teflon tubing (O.D. 550 μm, I.D. 400 μm, ∼20 cm in length) was inserted flush with the junction where aqueous plugs were formed (Fig. 2c). All the gaps between the PDMS channels and the Teflon tubing were sealed with wax to prevent leakage.

2.5 Forming LCP plugs in the flow-focusing device

LCP material was first made by mixing monoolein and Millipore water (w:w, 3:2) using an LCP mixer obtained from Emerald BioSystems, Inc. (Nollert 2002). Once the LCP material was formed, it was transferred into a syringe, and the mixer was disassembled. The syringe containing the LCP material was coupled to a 27-gauged syringe needle, which was connected to a piece of Teflon tubing (I.D. 300 μm, O.D. 750 μm, ∼5 cm in length). The LCP material was then transferred into the Teflon tubing. Once the tubing was filled, it was detached from the needle and was then attached to another 10 μl Hamilton glass syringe prefilled with FC-40. The tubing was then attached to the PDMS device, ready for forming LCP plugs.

2.6 Conditions for formation of LCP plugs

To determine the conditions for the formation of LCP plugs, the flow-focusing device was used without being connected to the merging device. A piece of Teflon tubing (O.D. 250 μm, I.D. 100 μm) was inserted flush with the cross junction via the outlet and the gap between the PDMS channel, and then the Teflon tubing was sealed with wax. At flow rates of the carrier fluid (FC-70) between 2 and 3 μl/min, LCP plugs formed successfully (Fig. 2e). All the solutions and LCP material in these experiments were loaded in glass syringes, and the flow rates were controlled by using syringe pumps from Harvard Apparatus.

2.7 Consistency of plug formation

To determine the consistency of the volume of the LCP plugs, the length of the plugs was monitored. In the same experiment, we also monitored the distance between plugs to determine the stability of flow in the device. In this experiment, the flow rates of LCP material and FC-70 were kept at 0.2 and 2 μl/min, respectively, and images of plugs were taken at a fixed position at nine different time points: 0, 2, 5, 9, 13, 16, 18, 23, and 28 min. For each time point, images of five different plugs were taken. The length of plugs in all images was then measured, as was the distance between two adjacent plugs (Fig. 3).

2.8 Stability of LCP plugs

To determine whether LCP material maintained its phase during formation of plugs, LCP plugs were formed, transported in Teflon tubing (100 μm I.D.), and imaged under cross-polarization. The flow rates were 0.3 μl/min for the LCP material and 2 μl/min for FC-70. After LCP plugs formed, the Teflon tubing was disconnected from the
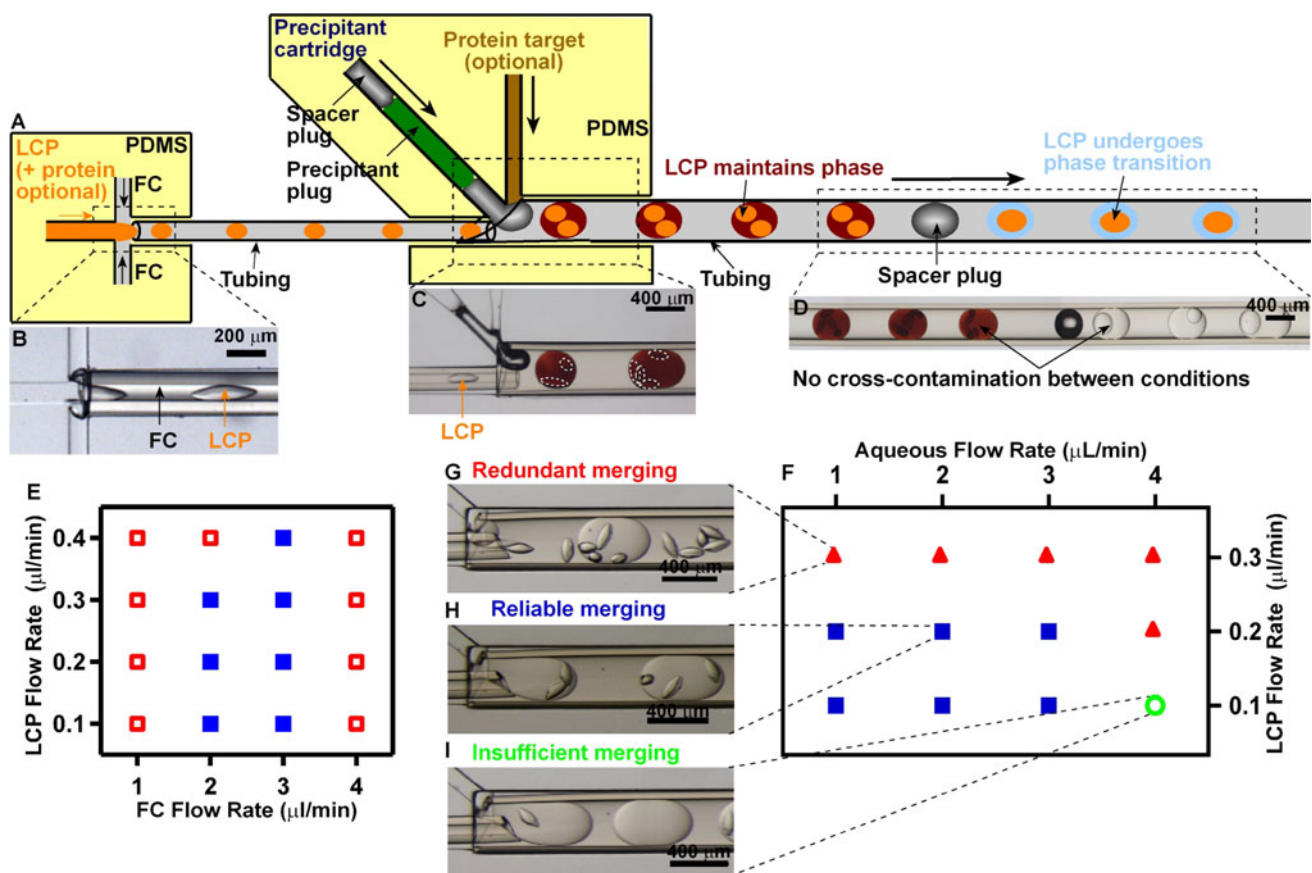
Fig. 2 Plug-based microfluidic system for crystallization of membrane proteins within lipidic mesophases. **a** A schematic of the microfluidic system. Small LCP plugs (~1 nl) were formed in a PDMS flow-focusing device using fluorinated carbon (FC) as a carrier fluid. The LCP plugs were transported in Teflon tubing, and then they merged downstream with the streams of protein and precipitant cartridges in a PDMS device to form LCP-containing aqueous plugs (~80 nl). The stream of protein was added only when LCP material was made using PLI (Fig. 1b). Upon merging with plugs containing certain precipitants, the LCP material may undergo phase transition to form another lipidic mesophase material, commonly known as a sponge phase (Wadsten et al. 2006). The plugs of the crystallization trials were stored and incubated at 23°C in Teflon tubing to allow crystals to grow. **b** A micrograph showing that LCP plugs formed in the flow-focusing device. **c** A micrograph showing that LCP plugs successfully merged with precipitant and protein solutions. LCP plugs are delineated by dashed white lines. **d** A micrograph showing that the plugs to the right of the air bubble did not contain red solution, indicating the absence of cross contamination of aqueous plugs separated by air bubbles (Li et al. 2006). **e** A phase diagram showing the working range of the flow rates of FC and LCP material that are required for reliably forming LCP plugs. The *solid squares* indicate reliable formation of LCP plugs, and the *open squares* indicate failure to form LCP plugs. **f** A phase diagram showing the flow rates of the LCP material and the aqueous flow rates that are required for reliable merging of LCP plugs with aqueous plugs. **g** A micrograph showing redundant merging caused by low aqueous flow rate and high LCP flow rate, indicated by *solid triangles* in the phase diagram. **h** A micrograph showing reliable merging at the working flow rates, indicated by the *solid squares* in the phase diagram. **i** A micrograph showing insufficient merging at high aqueous flow rate and low LCP flow rate, indicated by the *open circle* in the phase diagram

device and then the tubing was sealed at both ends. Images of plugs in the tubing were taken within 1 h under cross-polarized light (Fig. 4). We took images at two different angles of cross-polarized light to eliminate the possibility that background birefringence from the Teflon tubing could have hid any birefringence caused by the LCP material.

2.9 Merging LCP plugs with aqueous plugs

To determine whether LCP plugs could successfully merge with aqueous plugs in the microfluidic system, streams of 50% Polyethyleneglycol(PEG)-8000 and Millipore water were used as the precipitant stream and the protein stream, respectively, and LCP plugs were formed by using LCP materials made from monoolein and water, as described above. The flow rate of FC-70 was maintained at 3 μl/min throughout the experiment. A phase diagram was generated by using the total flow rate of aqueous solutions between 1 and 4 μl/min and using the flow rate of the LCP material between 0.1 and 0.3 μl/min (Fig. 2f–i). At a given total flow rate, each of the aqueous solutions flowed at a rate equal to half of the total flow rate.

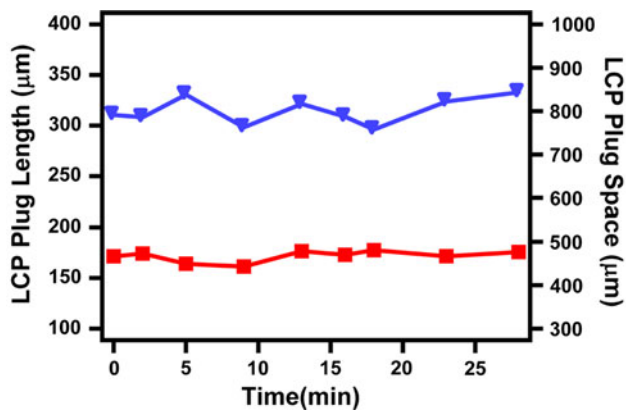**Fig. 3** LCP plugs formed consistently in the flow-focusing device. The flow rate of LCP material was 0.2 μl/min and the flow rate of FC-70 was 2 μl/min. The plug length (*solid squares*), which was directly correlated to the volume, was ~150 μm over more than 25 min. The standard deviation of the plug length was 8%, indicating that the standard deviation for the plug volume was 8%. The space between plugs (*solid triangles*) was ~800 μm over the same time period, with 16% variation
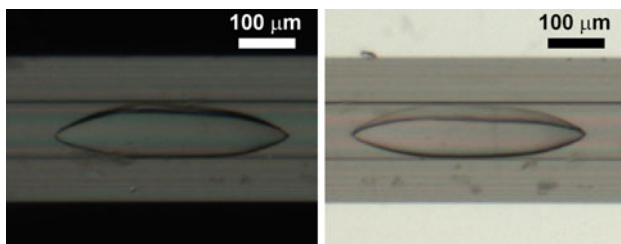

Fig. 4 LCP material maintained its phase during plug formation. Micrographs indicated the absence of birefringence of the LCP material at two different angles of cross-polarized light. Only background pattern, raised from the Teflon tubing, was observed

2.10 Forming cartridges for the precipitant stream

To determine whether cartridges can be implemented in the microfludic system, Millipore water was used as the protein stream, and a cartridge, consisting of 200 nl precipitant-mimicking plugs alternated with 50 nl air bubbles, was used as the precipitant stream. The cartridge contained 24 precipitant-mimicking plugs, of which 12 were colorless plugs, comprising conditions 1–12 from Hampton Research Index Screening Kit, and 12 were red plugs, containing 0.1 M Fe(SCN)$_3$ solution. The cartridge was prepared by alternating colorless plugs and red plugs. In the experiment, the flow rates of FC-70, the LCP material, the protein stream, and the precipitant stream were maintained at 3, 0.3, 0.5, and 1.5 μl/min, respectively. Images were recorded during and after the merging process (Fig. 2c, d).

2.11 Preparing samples of membrane proteins

Halobacterium salinarum S9 was grown using the published protocol (Cline and Doolittle 1987), and samples of bacteriorhodopsin (BR) were obtained by purification from membranes using the reported procedures (Nollert 2004) with separation proceeding on a GE Healthcare HiLoad™ 26/60 Superdex™ 75 Prep Grade column.

Carotenoid-containing and carotenoidless strains of *R. sphaeroides* were grown semi-aerobically in the dark in YCC Medium (Taguchi et al. 1992), and samples of poly-histidine-tagged RCs from *R. sphaeroides* were obtained by purification with minimal light exposure to a purity marked with optical absorbance ratio of $A_{800}/A_{280} \sim 1.5$ as previously described (Pokkuluri et al. 2002). Anion exchange chromatography (Tiede et al. 1996) was used to further improve purity of the samples and to increase crystallization reproducibility, bringing optical absorbance ratios of A_{800}/A_{280} to between 1.2 and 1.3.

Polyhistidine-tagged carotenoidless RCs were produced using a new expression strategy. A recombinant strain was created by mobilizing the expression vector pRKHTMHBgl (Pokkuluri et al. 2002), which carried a wild-type version of the gene encoding the L subunit and a modified version of the gene encoding the M subunit, into the host *R. sphaeroides* strain R26.1 (Theiler et al. 1984) via conjugation using the donor *E. coli* strain S17-1 (Simon et al. 1983). The new strain, R26.1[pRKHTMHBgl], simultaneously expressed tagged and untagged versions of the RC from *R. sphaeroides*. These two types of RCs were easily separated by metal affinity chromatography after being solubilized by using LDAO from intracytoplasmic membranes of the host strain.

2.12 Crystallizing BR

LCP material was made using the method described above (Nollert 2002), with the exception that Millipore water was replaced by a solution of BR sample. 30 mg monoolein and 20 μl BR, at a concentration of 22.5 mg/ml, were consumed to make the LCP material. Crystallization trials were set up in the microfludic system, which consisted of a flow-focusing device and a merging device bearing one aqueous inlet (Fig. 5c I). In the flow-focusing device, the flow rate of the carrier fluid, FC-70, was 3 μl/min, and the flow rate of the LCP material was 0.2 μl/min. Although the presence of detergents in a protein sample have an effect on LCP material (Ai and Caffrey 2000), we were still able to form LCP plugs in the presence of detergent (LDAO). Precipitant cartridges were used as the aqueous stream in the merging device. The cartridges consisted of 200 nl precipitant plugs alternated with 50 nl air bubbles.
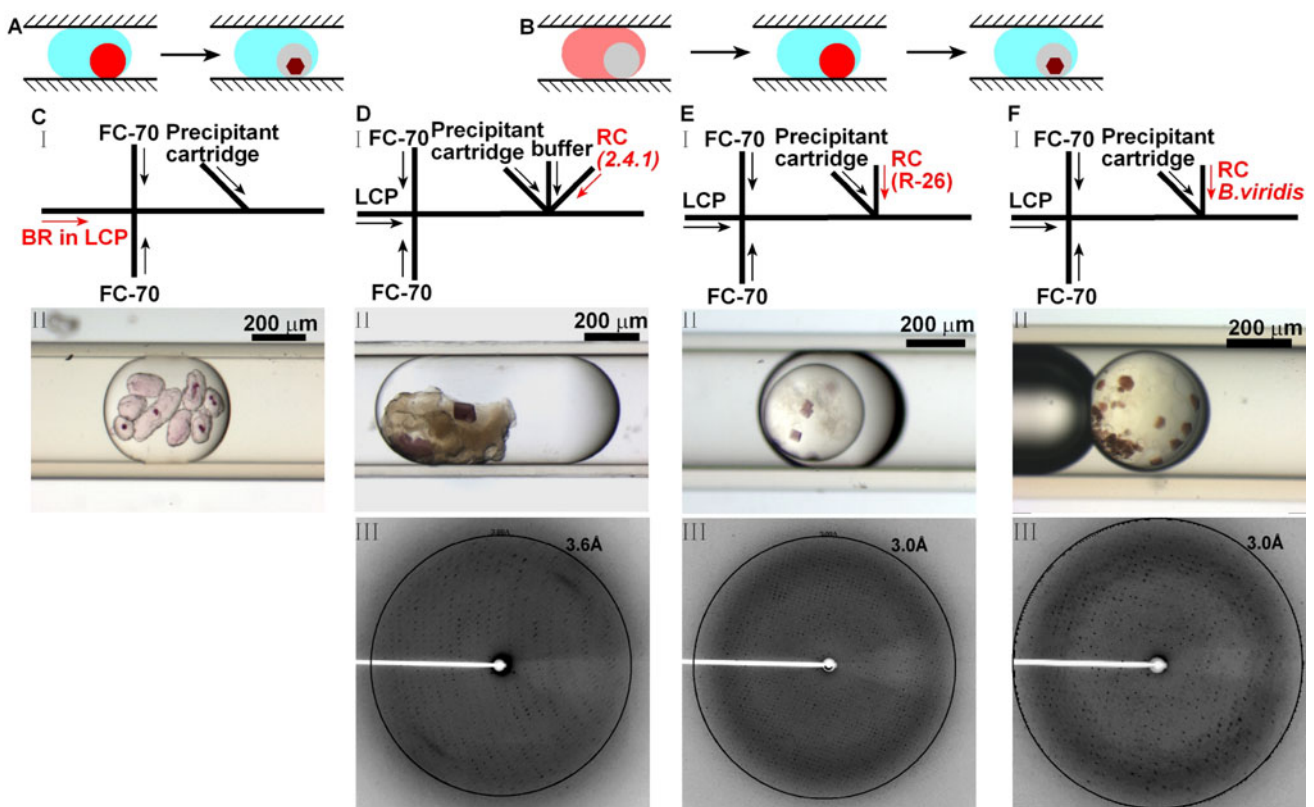
Fig. 5 **a** A schematic showing the traditional method for introducing protein into LCP material. **b** A schematic showing PLI, a method of forming LCP material without protein, adding the membrane protein sample externally to the LCP material, and allowing the protein to diffuse into the LCP material. **c** Crystallization of BR using the traditional method. **c**, I—A schematic showing the experimental setup for crystallization. **c**, II—A plug with crystals (in *dark spots*) of BR (from *H. salinarum*) obtained when BR was premixed in LCP material. **d**, **e**, **f** Crystallization of three proteins using PLI. (I) Schematics showing the experimental setups for crystallization using PLI. For the carotenoid-containing RC from *R. sphaeroides* (**d**, I), additional buffer was added to the precipitant cartridge and protein streams. For the carotenoidless RC from *R. sphaeroides* (**e**, I) and RC from *B. viridis* (**f**, I), no additional buffer was added to the precipitant cartridge and protein streams. (II) Plugs with crystals obtained using PLI of (**c**, II) carotenoid-containing RC, (**d**, II) carotenoidless RC, and (**e**, II) RC (*B. viridis*). (III) Diffraction-quality crystals were obtained from proteins grown in lipidic mesophase material. **c**, III—A crystal of carotenoid-containing RC diffracted X-ray to ∼3.5 Å (ring indicates 3.6 Å resolution). **d**, III—A crystal of carotenoidless RC grown in lipidic mesophase material diffracted X-ray to ∼2.5 Å (ring indicates 3.0 Å resolution). **e**, III—A crystal of RC (*B. viridis*) diffracted X-ray to ∼2.8 Å (ring indicates 3.0 Å resolution)

Two cartridges, each containing 25 conditions from Crystal Screen kit (Hampton Research), were prepared as previously reported (Li et al. 2006), resulting in 50 total conditions. The cartridges were flowed at a rate of 2.0 μl/min. Once the crystallization trials were set up, the Teflon tubing containing the trials was detached from the network and sealed in a piece of glass tubing prefilled with FC-70. The trials were then incubated at 23°C in the dark.

2.13 Crystallizing carotenoid-containing RC

LCP material was made using the method described above (Nollert 2002). 30 mg monoolein and 20 μl Millipore water were used to make the LCP material.

Crystallization trials were set up in the microfluidic system, which included a flow-focusing device and a merging device bearing three aqueous inlets (Fig. 5d I): the first for precipitant cartridges, the second for the buffer (0.05% (w/v) LDAO, 10 mM Tris pH 7.8), and the third for the protein sample (20 mg/ml in 0.05% (w/v) LDAO, 10 mM Tris pH 7.8). The precipitant cartridges were made in the same way as described above, except that a different kit, provided by Emerald Biosystems, was used to prepare 48 different conditions (Table S1). The carrier fluid, FC-70, was flowed at a rate of 3 μl/min; the flow rate of LCP material was 0.3 μl/min. The flow rates of the precipitant cartridge, the buffer, and the protein sample were 1.5, 0.1, and 0.5 μl/min, respectively. The trials were incubated as described above. Crystals began to appear within a week.

2.14 Crystallizing carotenoidless RC

The same procedure that was followed for crystallizing carotenoid-containing RC was followed for crystallizing carotenoidless RC. In this case, however, the merging device contained only two aqueous inlets (Fig. 5e I): one for precipitant cartridges, flowing at a rate of 1.8 μl/min, and the other for the protein sample (20 mg/ml in 0.05% (w/v) LDAO, 10 mM Tris pH 7.8), flowing at a rate of 0.2 μl/min. The same screening kit, provided by Emerald Biosystems, as was used for crystallizing carotenoid-containing RC was also used here. The trials were incubated as described above. Crystals began to appear within 2 days.

2.15 Crystallizing RC from *B. viridis*

The same procedure that was followed for crystallizing carotenoidless RC was followed for crystallizing RC from *B. viridis* (Fig. 5f I). The protein sample was 26 mg/ml in 0.08% (w/v) LDAO, 50 mM Na_2PO_4–NaH_2PO_4, pH 6.0. The same screening kit and incubation procedures were used. Crystals began to appear within a week.

2.16 Preparing crystals for X-ray diffraction

Crystallization trials were checked by using a stereoscope under minimal light. The same procedure as previously reported (Li et al. 2006) was followed, and plugs containing crystals were flowed into a droplet of the mother liquor sitting in a microwell. No cryoprotectant was needed. Crystals, together with the lipidic mesophase material, were looped from droplets directly and were then flash frozen in liquid nitrogen.

2.17 X-ray diffraction and data processing

X-ray diffraction was performed at GM/CA Cat station 23 ID-B of the Advanced Photon Source (Argonne National Laboratory). The data were processed in HKL2000 (Otwinowski and Minor 1997).

3 Results and discussion

3.1 LCP material reliably formed nanoliter-volume plugs

First, we demonstrated the compatibility of LCP material with the plug-based microfluidic system (Fig. 2). LCP plugs were first formed in a microfluidic stream (Fig. 2a). The working flow rates in these experiments are shown in a phase diagram (Fig. 2e). The minimum working flow rate was limited by the viscosity of the LCP material. At flow rates of FC of 2 μl/min or higher, the cross flow of the FC provided shear high enough to cut the viscous LCP stream into nanoliter-volume plugs (Fig. 2b). The maximum working flow rate was limited by the maximum pressure the device could withstand, ∼0.4 MPa (McDonald et al. 2000). At flow rates of FC of 4 μl/min or higher, the pressure on the device was greater than 0.4 MPa. The volume of the LCP plugs, ∼1 nl, was consistent over time with a standard deviation of 8% (Fig. 3). We checked the stability of LCP material in the carrier fluid in a separate experiment, and the LCP material maintained its phase while forming plugs (Fig. 4).

3.2 LCP plugs successfully merged with aqueous plugs to create crystallization trials without cross contamination

When the LCP plugs came in contact with the aqueous plugs, they merged with the aqueous plugs, presumably to minimize interfacial energy due to the hydrophilic surface of the LCP material. In the presence of certain precipitants, the LCP material in the merged plugs may undergo a phase transition to form another lipidic mesophase, commonly known as a sponge phase (Fig. 2a, d). The efficiency of merging of LCP plugs with aqueous plugs for the crystallization trials was governed by the flow rate of the LCP material upstream and the aqueous flow rate at which the plugs for crystallization trials were formed (Fig. 2f). To describe this effect, we defined the frequency f_1 as the number of LCP plugs that were formed upstream per second and the frequency f_2 as the number of aqueous plugs of crystallization trials that were formed per second. The ratio, $N = f_1/f_2$, denotes the number of LCP plugs in each aqueous plug and defines the efficiency of merging. The lower limit of N is 1, because every aqueous plug must merge with at least one LCP plug, and the upper limit of N is set by the requirement that a single aqueous plug must accommodate all the LCP plugs formed upstream. When the flow rate of LCP material and the aqueous solution was moderate (flow rate of LCP material = 0.1 or 0.2 μl/min; aqueous flow rate = 1, 2, or 3 μl/min), N was greater than 1 but less than 8, and reliable merging was observed (Fig. 2f, solid squares, h). When the flow rate of the LCP material was too high (0.3 μl/min or higher), f_1 increased and so did N, up to values over 8. This resulted in redundant merging, in which more than one LCP plug merged with each aqueous plug (Fig. 2f, solid triangles, and g). When the aqueous flow rate was too high (over 4 μl/min), f_2 increased, and N dropped below 1. At low LCP flow rates, the LCP material could not reliably merge with every aqueous plug, resulting in insufficient merging (Fig. 2f, open circles, and i), and at higher LCP flow rates redundant merging was again observed.

Under the working conditions described above, the LCP plugs preferentially merged with the aqueous plugs, and each merged plug constituted a crystallization experiment with no cross contamination between conditions (Fig. 2d). This method allowed for sparse matrix screening of crystallization conditions with LCP material.

3.3 Model membrane proteins crystallized using the plug-based LCP-assisted microfluidic system

Having demonstrated the compatibility of the plug-based microfluidic system with LCP material, we then validated the system by crystallizing proteins (Table 1) using the two different methods of introducing membrane protein into LCP material (Fig. 1).

To test the compatibility of our system with method 1 (Fig. 5a), we selected BR from *H. salinarum*, and we prepared the LCP material by directly mixing monoolein with a solution of BR (3:2 (w/w) ratio). In this experiment, the aqueous stream was a single stream, containing an array of precipitant plugs (Fig. 5c I). Conditions were screened using a commercial kit (Crystal Screen from Hampton Research) and crystals were obtained (Fig. 5d) in 16 different conditions (Table 1, the specific conditions are listed in Table S2). Thus, the traditional method for making LCP material with protein was successfully implemented in the plug-based system. Although BR crystals were too small to be characterized by X-ray diffraction, the crystals were identified by the color of the protein and the shape of the potential crystal (Fig. 5c II).

To demonstrate PLI, three target proteins were screened against conditions formed with various combinations of Jeffamine M-600 and $(NH_4)_2SO_4$ (Table S1), 48 different conditions in total. The targets were membrane proteins with known crystallization conditions that included RCs from two bacterial species: *R. sphaeroides* and *B. viridis*. In the experimental configurations for all targets, proteins could be conveniently injected as an aqueous stream laminar with the stream containing the precipitant cartridge (Fig. 5d I, e I, f I). The precipitant cartridge contained an array of aqueous precipitant plugs ($\sim$200 nl in volume) separated by air bubbles ($\sim$50 nl in volume); each precipitant plug contained unique conditions for protein crystallization. In these crystallization experiments, each precipitant plug formed three to four smaller aqueous plugs that then merged with the LCP plugs; the plugs formed in this way from a single precipitant plug constituted replicate crystallization trials of a given condition. Thus, with a protein sample of $\sim$3 µl, 48 different conditions, with 3–4 replicates each, could be set up within 6 min.

Some of the LCP plugs, upon merging with aqueous plugs containing precipitant and protein, underwent a phase transition to another lipidic mesophase (Cherezov et al. 2006; Cherezov et al. 2001). Crystals grew directly in the new lipidic mesophase material (Fig. 5d II, e II, f II). Crystals of carotenoid-containing RC from *R. sphaeroides 2.4.1* formed (Fig. 5d II) in the mesophase within a week in 3 of 48 conditions (Table 1, the specific conditions are listed in Table S1) and diffracted X-rays to $\sim$3.5 Å (Fig. 5d III). Crystals of caroteniodless RC from *R. sphaeroides R26* formed (Fig. 5e II) in the lipidic mesophase material within 2 days in 16 of 48 conditions (Table 1, the specific conditions are listed in Table S1) and diffracted X-rays to $\sim$2.5 Å (Fig. 5e III). Crystals of RC from *B. viridis* formed (Fig. 5f II) in the lipidic mesophase material within a week in 6 of 48 conditions (Table 1, the specific conditions are listed in Table S1) and diffracted X-rays to $\sim$2.8 Å (Fig. 5f III).

Crystals of carotenoidless RC from *R. sphaeroides R26* obtained by using PLI (Fig. 5e III) belonged to $P4_22_12$ with the unit cell parameter of $a = b = 101.0$ Å, $c = 238.4$ Å; $\alpha = \beta = \gamma = 90°$. These results were similar to those obtained previously by forming LCP material with protein (Katona et al. 2003), validating the PLI method. The consistency in the unit cell parameter between the results obtained here and those reported previously may imply that crystallization occurred after RC diffused into the lipidic mesophase when PLI was used. That is, the same crystal morphology may be due to crystallization in both cases sharing the same mechanism.

4 Conclusion

We developed a plug-based microfluidic system that accurately dispenses nanoliter volumes of lipidic cubic phase (LCP) material. LCP material formed plugs of nanoliter volumes with 8% deviation in length among plugs. Conditions for the formation of LCP plugs were

Table 1 Summary of crystallization experiments using membrane protein targets in the plug-based LCP-assisted microfluidic system

Protein	Source	M.W. (kDa)	Detergent (mM)	Protein (mg/ml)	Crystallization hits out of 48 precipitants
Bacteriorhodopsin	*H. salinarum*	27	40	12–30	16
Carotenoid-containing reaction center	*R. sphaeroides 2.4.1 derivative*	100	2	10–25	3
Carotenoidless reaction center	*R. sphaeroides R26*	100	2	$\sim$20	16
Reaction center with bound cytochrome	*B. viridis*	135	3.5	$\sim$20	6

characterized and presented in a phase diagram. We validated this system by successfully screening conditions for crystallization of membrane proteins; each crystallization plug constituted an individual experiment under different conditions. The system we have described is compatible with the traditional method of pre-forming LCP material using a membrane protein sample, as well as with PLI, a method of forming LCP material without protein, adding the membrane protein sample externally to the LCP material, and allowing the protein to diffuse into the LCP material. Because PLI relies on diffusion of the protein into the LCP material, it may be limited by any factors that limit this diffusion, such as the size of the protein. We will test a batch of membrane proteins with different sizes of hydrophilic areas in future studies. Nevertheless, this alternative approach eliminated the step of preparing LCP material individually for every protein target studied. This alternative method minimizes sample consumption because the protein samples can be filled into syringes without loss in dead volumes. The volumes used in this system could potentially be scaled down further: Using the current device with the pressure limit of 0.4 MPa, LCP plugs as small as 200 pL should be formed at a total flow rate of 0.4 µl/min in a 7 cm long piece of Teflon tubing with 60 µm I.D. Furthermore, by adding extra inlets for aqueous streams, the system could be made compatible with more complicated methods of screening, such as additive methods and those using ligands. This method should complement current developments in LCP-based microscale protein crystallization (Cherezov and Caffrey 2006; Peddi et al. 2007; Perry et al. 2009).

References

Ai X, Caffrey M (2000) Membrane protein crystallization in lipidic mesophases: detergent effects. Biophys J 79(1):394–405

Caffrey M (2000) A lipid's eye view of membrane protein crystallization in mesophases. Curr Opin Struct Biol 10(4):486–497

Cherezov V, Caffrey M (2006) Picolitre-scale crystallization of membrane proteins. J Appl Crystallogr 39:604–606

Cherezov V, Fersi H, Caffrey M (2001) Crystallization screens: compatibility with the lipidic cubic phase for in meso crystallization of membrane proteins. Biophys J 81(1):225–242

Cherezov V, Peddi A, Muthusubramaniam L, Zheng YF, Caffrey M (2004) A robotic system for crystallizing membrane and soluble proteins in lipidic mesophases. Acta Crystallogr D 60:1795–1807

Cherezov V, Clogston J, Papiz MZ, Caffrey M (2006) Room to move: crystallizing membrane proteins in swollen lipidic mesophases. J Mol Biol 357(5):1605–1618

Cherezov V, Rosenbaum DM, Hanson MA, Rasmussen SGF, Thian FS, Kobilka TS, Choi HJ, Kuhn P, Weis WI, Kobilka BK, Stevens RC (2007) High-resolution crystal structure of an engineered human beta(2)-adrenergic G protein-coupled receptor. Science 318(5854):1258–1265

Cline SW, Doolittle WF (1987) Efficient transfection of the archaebacterium *Halobacterium halobium*. J Bacteriol 169(3):1341–1344

Davis J, Donohue TJ, Kaplan S (1988) Construction, characterization, and complementation of a Puf- mutant of *Rhodobacter sphaeroides*. J Bacteriol 170(1):320–329

Duffy DC, McDonald JC, Schueller OJA, Whitesides GM (1998) Rapid prototyping of microfluidic systems in poly(dimethylsiloxane). Anal Chem 70(23):4974–4984

Jaakola VP, Griffith MT, Hanson MA, Cherezov V, Chien EYT, Lane JR, Ijzerman AP, Stevens RC (2008) The 2.6 angstrom crystal structure of a human A(2A) adenosine receptor bound to an antagonist. Science 322(5905):1211–1217

Katona G, Andreasson U, Landau EM, Andreasson LE, Neutze R (2003) Lipidic cubic phase crystal structure of the photosynthetic reaction centre from *Rhodobacter sphaeroides* at 2.35 angstrom resolution. J Mol Biol 331(3):681–692

Lau BTC, Baitz CA, Dong XP, Hansen CL (2007) A complete microfluidic screening platform for rational protein crystallization. J Am Chem Soc 129(3):454–455

Li L, Mustafi D, Fu Q, Tereshko V, Chen DLL, Tice JD, Ismagilov RF (2006) Nanoliter microfluidic hybrid method for simultaneous screening and optimization validated with crystallization of membrane proteins. Proc Natl Acad Sci USA 103(51):19243–19248

McDonald JC, Duffy DC, Anderson JR, Chiu DT, Wu HK, Schueller OJA, Whitesides GM (2000) Fabrication of microfluidic systems in poly(dimethylsiloxane). Electrophoresis 21(1):27–40

Nollert P (2002) From test tube to plate: a simple procedure for the rapid preparation of microcrystallization experiments using the cubic phase method. J Appl Crystallogr 35:637–640

Nollert P (2004) Lipidic cubic phases as matrices for membrane protein crystallization. Methods 34(3):348–353

Ostermeier C, Michel H (1997) Crystallization of membrane proteins. Curr Opin Struct Biol 7(5):697–701

Otwinowski Z, Minor W (1997) Processing of X-ray diffraction data collected in oscillation mode. In: Carter CW, Sweet RM (eds) Macromolecular crystallography, Pt A, vol 276, Academic Press Inc., San Diego, pp 307–326

Peddi A, Muthusubramaniam L, Zheng YR, Cherezov V, Misquitta Y, Caffrey M (2007) High-throughput automated system for crystallizing membrane proteins in lipidic mesophases. IEEE Trans Autom Sci Eng 4(2):129–140

Perry SL, Roberts GW, Tice JD, Gennis RB, Kenis PJA (2009) Microfluidic generation of lipidic mesophases for membrane protein crystallization. Cryst Growth Des 9(6):2566–2569

Pokkuluri PR, Laible PD, Deng YL, Wong TN, Hanson DK, Schiffer M (2002) The structure of a mutant photosynthetic reaction center shows unexpected changes in main chain orientations and quinone position. Biochemistry 41(19):5998–6007

Roach LS, Song H, Ismagilov RF (2005) Controlling nonspecific protein adsorption in a plug-based microfluidic system by controlling interfacial chemistry using fluorous-phase surfactants. Anal Chem 77(3):785–796

Shestopalov I, Tice JD, Ismagilov RF (2004) Multi-step synthesis of nanoparticles performed on millisecond time scale in a microfluidic droplet-based system. Lab Chip 4(4):316–321

Shim JU, Cristobal G, Link DR, Thorsen T, Jia YW, Piattelli K, Fraden S (2007) Control and measurement of the phase behavior of aqueous solutions using microfluidics. J Am Chem Soc 129(28):8825–8835

Simon R, Priefer U, Puhler A (1983) A broad host range mobilization system for invivo genetic-engineering: transposon mutagenesis in gram-negative bacteria. Bio-Technology 1(9):784–791

Song H, Tice JD, Ismagilov RF (2003) A microfluidic system for controlling reaction networks in time. Angew Chem Int Ed 42(7):768–772

Song H, Chen DL, Ismagilov RF (2006a) Reactions in droplets in microflulidic channels. Angew Chem Int Ed 45(44):7336–7356

Song H, Li HW, Munson MS, Van Ha TG, Ismagilov RF (2006b) On-chip titration of an anticoagulant argatroban and determination of the clotting time within whole blood or plasma using a plug-based microfluidic system. Anal Chem 78(14):4839–4849

Taguchi AK W, Stocker JW, Alden RG, Causgrove TP, Peloquin JM, Boxer SG, Woodbury NW (1992) Biochemical-characterization and electron-transfer reactions of Sym1, a *Rhodobacter capsulatus* reaction center symmetry mutant which affects the initial electron-donor. Biochemistry 31(42):10345–10355

Theiler R, Suter F, Zuber H, Cogdell RJ (1984) A comparison of the primary structures of the 2 B800–850-apoproteins from wild-type *Rhodopseudomonas sphaeroides* strain 2.4.1 and a carotenoidless mutant strain R26.1. FEBS Lett 175(2):231–237

Tiede DM, Vazquez J, Cordova J, Marone PA (1996) Time-resolved electrochromism associated with the formation of quinone anions in the *Rhodobacter sphaeroides* R26 reaction center. Biochemistry 35(33):10763–10775

Toepke MW, Beebe DJ (2006) PDMS absorption of small molecules and consequences in microfluidic applications. Lab Chip 6(12):1484–1486

Wadsten P, Wohri AB, Snijder A, Katona G, Gardiner AT, Cogdell RJ, Neutze R, Engstrom S (2006) Lipidic sponge phase crystallization of membrane proteins. J Mol Biol 364(1):44–53

Wohri AB, Johansson LC, Wadsten-Hindrichsen P, Wahlgren WY, Fischer G, Horsefield R, Katona G, Nyblom M, Oberg F, Young G, Cogdell RJ, Fraser NJ, Engstrom S, Neutze R (2008) A lipidic-sponge phase screen for membrane protein crystallization. Structure 16(7):1003–1009

Zheng B, Roach LS, Ismagilov RF (2003) Screening of protein crystallization conditions on a microfluidic chip using nanoliter-size droplets. J Am Chem Soc 125(37):11170–11171

Zheng B, Gerdts CJ, Ismagilov RF (2005) Using nanoliter plugs in microfluidics to facilitate and understand protein crystallization. Curr Opin Struct Biol 15(5):548–555